ANL/FPP/TM-281
ITER/US/95/IV-BL-05

ANL/FPP/TM-281
ITER/US/95/IV-BL-05

SUMMARY REPORT FOR ITER TASK – T19: MHD PRESSURE DROP AND HEAT TRANSFER STUDY FOR LIQUID METAL SYSTEMS

by

C. B. Reed, T. Q. Hua, K. Natesan, I. R. Kirillov,
I. V. Vitkovski, and A. M. Anisimov

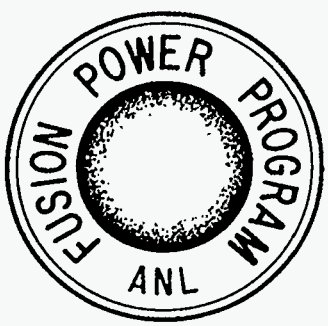

FUSION POWER PROGRAM

Argonne National Laboratory
9700 South Cass Avenue
Argonne, Illinois 60439

Operated by
The University of Chicago
for the U.S. Department of Energy
under Contract W-31-109-Eng-38

Distribution Category
Magnetic Fusion Energy Systems
(UC-424)

ANL/FPP/TM-281

ITER/US/95/IV-BL-05

ARGONNE NATIONAL LABORATORY
9700 South Cass Avenue
Argonne, Illinois 60439-4801 USA

SUMMARY REPORT FOR ITER TASK - T19: MHD PRESSURE DROP AND HEAT TRANSFER STUDY FOR LIQUID METAL SYSTEMS

by

Claude B. Reed and Thanh Q. Hua
Fusion Power Program/Technology Development Division

Ken Natesan
Fusion Power Program/ Energy Technology Division

Igor R. Kirillov, Ivan V. Vitkovski, and Aleksandr M. Anisimov
MHD-Machines Laboratory
The D.V. Efremov Scientific Research
Institute of Electrophysical Apparatus
189631 St. Petersburg, Russia

March 1995

Work supported by the
Office of Fusion Energy
U.S. Department of Energy
under Contract W-31-109-Eng-38

TABLE OF CONTENTS

LIST OF FIGURES

SUMMARY REPORT FOR ITER TASK - T19: MHD PRESSURE DROP AND HEAT TRANSFER STUDY FOR LIQUID METAL SYSTEMS

Claude B. Reed, Ken Natesan, Thanh Q. Hua, Igor R. Kirillov,
Ivan V. Vitkovski, and Aleksandr M. Anisimov

ABSTRACT

A key feasibility issue for the ITER Vanadium/Lithium breeding blanket is the question of insulator coatings. Design calculations show that an electrically insulating layer is necessary to maintain an acceptably low MHD pressure drop. To begin experimental investigations of the MHD performance of candidate insulator materials and the technology for putting them in place, a new test section was prepared. Aluminum oxide was chosen as the first candidate insulating material because it may be used in combination with NaK in the ITER vacuum vessel and/or the divertor; and MHD performance tests could begin early in ALEX (Argonne's Liquid Metal EXperiment) because NaK was already the working fluid in use.

Details on the methods used to produce the aluminum oxide layer as well as the microstructures of the coating and the aluminide sublayer are presented and discussed.

The overall MHD pressure drop, local MHD pressure gradient, local transverse MHD pressure difference, and surface voltage distributions in both the circumferential and the axial directions are reported and discussed. The overall MHD pressure drop, measured at 30, 85, and 200°C, was higher than the perfectly insulating case, but many times lower than the bare wall case.

The positive results obtained here for high-temperature NaK have two beneficial implications for ITER. First, since NaK may be used in the vacuum vessel and/or the divertor, these results support the design approach of using electrically insulating coatings to substantially reduce MHD pressure drop. Secondly, while Al_2O_3/SS is not the same coating/base material combination which would be used in the advanced blanket, this work nonetheless shows that it is possible to produce a viable insulating coating which is stable in contact with a high temperature alkali metal coolant.

Summary

A key feasibility issue for the ITER Vanadium/Lithium breeding blanket is the question of insulator coatings. Design calculations show that an electrically insulating layer is necessary to maintain an acceptably low MHD pressure drop. To begin experimental investigations of the MHD performance of candidate insulator materials and the technology for putting them in place, a new test section was prepared. Aluminum oxide was chosen as the first candidate insulating material because it may be used in combination with NaK in the ITER vacuum vessel and/or the divertor; and MHD performance tests could begin early in ALEX (Argonne's Liquid Metal Experiment) because NaK was already the working fluid in use.

Details on the methods used to produce the aluminum oxide layer as well as the microstructures of the coating and the aluminide sublayer are presented and discussed.

The overall MHD pressure drop, local MHD pressure gradient, local transverse MHD pressure difference, and surface voltage distributions in both the circumferential and the axial directions are reported and discussed. The overall MHD pressure drop, measured at 30, 85, and 200°C, was higher than the perfectly insulating case, but many times lower than the bare wall case. It was demonstrated that the increase in MHD pressure drop above the theoretical values is due largely to the presence of instrumentation penetrations in the test section walls, which provide current paths from the fluid to the walls of the pipe, resulting in local areas of near-bare-wall MHD pressure drop.

The positive results obtained here for high-temperature NaK have two beneficial implications for ITER. First, since NaK may be used in the vacuum vessel and/or the divertor, these results support the design approach of using electrically insulating coatings to substantially reduce MHD pressure drop. Electrically insulating coatings are, therefore, no longer a feasibility issue in these two components. Secondly, while Al_2O_3/SS is not the same coating/base material combination which would be used in the advanced blanket, this work nonetheless shows that it is possible to produce a viable insulating coating which is stable in contact with a high temperature alkali metal coolant.

1. Introduction

A key feasibility issue for the ITER Vanadium/Lithium breeding blanket is the question of insulator coatings. Design calculations, Hua and Gohar [1], show that an electrically insulating layer is necessary to maintain an acceptably low MHD pressure drop.

The goals of this task were to:

- apply an electrically insulating coating to the inside surface of a large-scale component,
- show that the coating on the component is compatible with a high-temperature liquid metal (NaK at 200°C),
- demonstrate that the coating produces a significant reduction in the MHD pressure drop, comparable to a perfectly insulating coating, and
- compare the results to pre-test predictions.

To begin experimental investigations of the MHD performance of candidate insulator materials and the technology for putting them in place, a new test section was prepared as follows. A round pipe of Type 304 stainless steel was aluminized on the inside surface, resulting in a layer of Fe-Al alloy 50-100 μm thick. A commercially available high temperature packed powder process was used. The resultant aluminum rich surface layer was subsequently oxidized in air at 980°C for 4 h, followed by a slow cool in air to room temperature. The end product was a stainless steel tube having an aluminum oxide layer on the inside surface which was a few micrometers thick. Aluminum oxide was chosen as the first candidate insulating material because it may be used in combination with NaK in the ITER vacuum vessel and/or the divertor; and MHD performance tests could begin early in ALEX (Argonne's Liquid Metal EXperiment) because NaK was already the working fluid in use. Future testing will move toward Vanadium ducts with an appropriate insulating layer.

The inside diameter of the pipe was 10.8 cm, the wall thickness was 2.9 mm, the length of the uniform magnetic field was approximately 1.8 m, and the maximum magnetic field strength was 2.0 T. The highest Hartmann number (M) and interaction parameter (N, using the pipe radius as the characteristic length) are 9200 and 10^4, respectively, at which reliable MHD pressure drop measurements were made. Each of these values is within one order of magnitude of ITER-relevant conditions. A movable electrode device consisting of arrays of electrodes was mounted on the outside surface of the pipe. This device was used as a diagnostic tool to assess the impact of any imperfections which may exist in the insulating layer. Any non zero voltages measured by the electrodes are an indication of leakage current flowing in the walls of the test section. Measurements were gathered in the uniform field and fringing field regions. Results of MHD pressure drop measurements and electric potential profiles acquired from this first insulated wall test section under a wide variety of conditions produced by varying the magnetic field, flow rate, operating temperature, and operating time at temperature are presented and compared with ANL pre-test predictions.

2. Description of Coating Achieved on Inside Surface of Test Section

Extensive thermodynamic calculations have been made to evaluate potential electrical insulator candidates that are (a) chemically compatible in liquid metals and (b) possess adequate insulating characteristics for use as a coating on the first-wall and blanket structural material. A review of available information on the electrical resistivity values for several oxides, nitrides, and oxynitrides showed that a number of oxides (e.g., CaO, MgO, SiO_2, Al_2O_3, $MgAl_2O_4$) and nitrides (e.g., AlN, Si_3N_4) have resistivities greater than 10^5 Ohm-m at temperatures below approximately 600°C, Natesan et al. [2]. The requirement is that the product of insulator coating electrical resistivity and thickness should exceed a nominal value of 0.024 Ohm m^2, Hua and Gohar [1], under ITER operating and geometric conditions. Based on the resistivity values of materials listed above, a coating layer of 1-10 μm thick of any of these materials would be several orders of magnitude higher than the requirement. Radiation effects will reduce this margin because of resistivity degradation. An experimental program is under way to quantify the radiation effects. To validate the effect of insulated pipe on the MHD pressure drop, eutectic alloy of Na-78 wt.%K and alumina coating on a Type 304 stainless steel pipe are used in the

present study. Figure 1 shows a comparison of resistance of several oxide materials, together with the requirements for ITER application.

The alumina coating has been applied using a pack diffusion method. In the pack process, the substrate material is contacted and heated for 4-12 h at temperatures of approximately 900°C with a pack of powders. The composition of such powders (e.g., 65 wt.% Al_2O_3, 33 wt.% Al, 2 wt.% NH_4Cl) provides the packing with metallic Al, alumina as filler material, and NH_4Cl as activator. The amount of Al can be reduced by partly replacing with Ni. The Al deposited on the substrate surface diffuses into the subsurface regions of the material, where it forms intermetallic phases as aluminides of Fe or Ni. Since the substrate materials are heated to temperatures close to the annealing range for times sufficient to cause solution processes in the matrix, the materials need a final treatment in order to optimize the structure. The aluminide layers reach thicknesses of 0.025-0.20 mm, depending on the composition of the substrate materials. Figure 2 shows the elemental concentration profiles for Type 304 stainless steel in as-aluminized condition. The aluminum concentration can reach 50 wt.% or more over a depth of approximately 160 μm from the surface beyond which the Al concentration decreases to zero at a depth of about 440 μm.

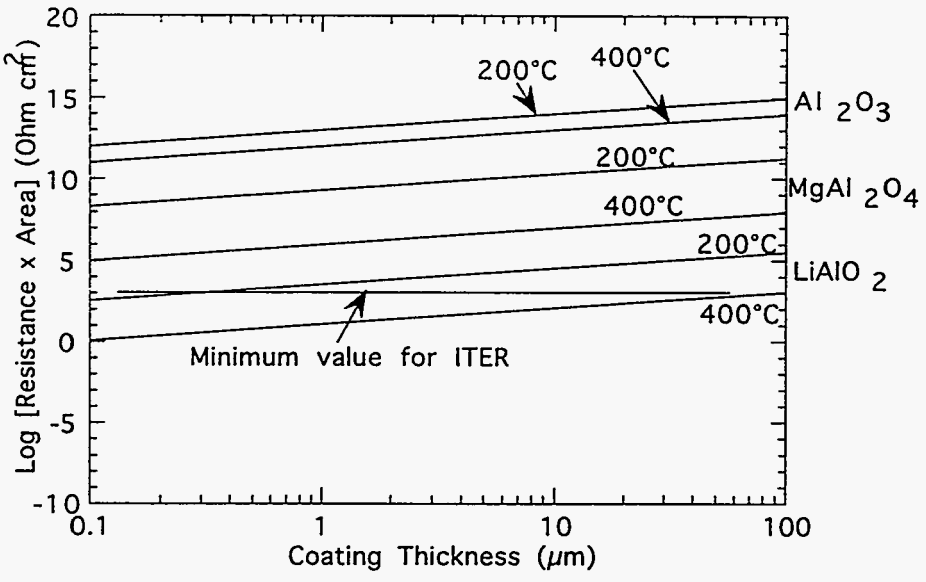

Fig. 1 Resistance of several oxides as a function of coating thickness; requirements for ITER application shown for reference.

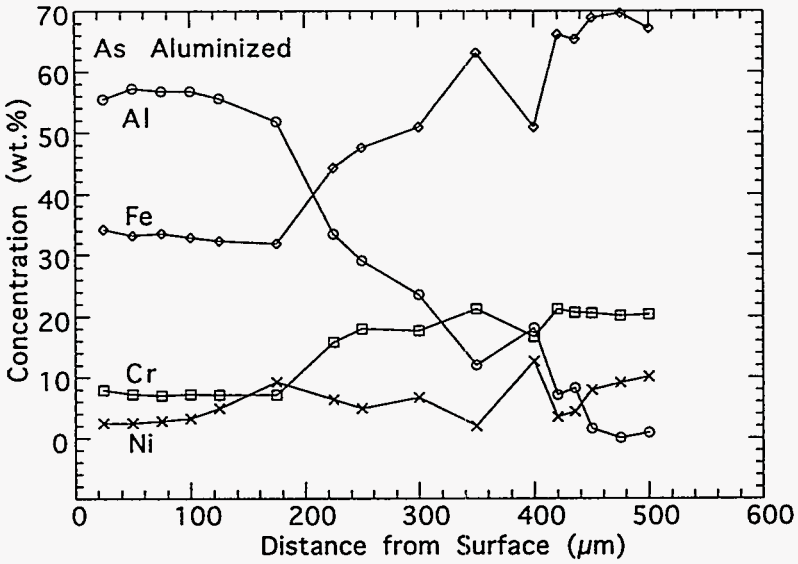

Fig. 2 Typical elemental concentration profiles for Al, Fe, Cr, and Ni for Type 304 stainless steel in the as aluminized condition.

After aluminizing using the above procedure, the pipes needed to be oxidized at elevated temperature for a time period sufficient to develop an adherent alumina layer with adequate insulating properties. To establish the optimum time for oxidation, specimens of aluminized pipe were exposed to an air environment for time periods of 4, 8, 12, 24, and 48 h at 982°C. Detailed analysis of the surfaces and cross sections of the exposed specimens were conducted using scanning electron microscopy (SEM) and it was concluded that 4 h exposure will be optimum for developing an insulating layer of alumina. Figure 3 shows the SEM photomicrographs of specimens exposed to air at 982°C for 4, 8, 12, and 24 h. Even though the depth of aluminized layer is of the order of 160 μm with a gradient to 440 μm, the thickness of oxide layer after 4 h was only of the order of 2-5 μm which is more than adequate from the insulating standpoint. Figure 4 shows SEM photomicrographs of three different locations of the pipe after 4 h exposure to air at 982°C.

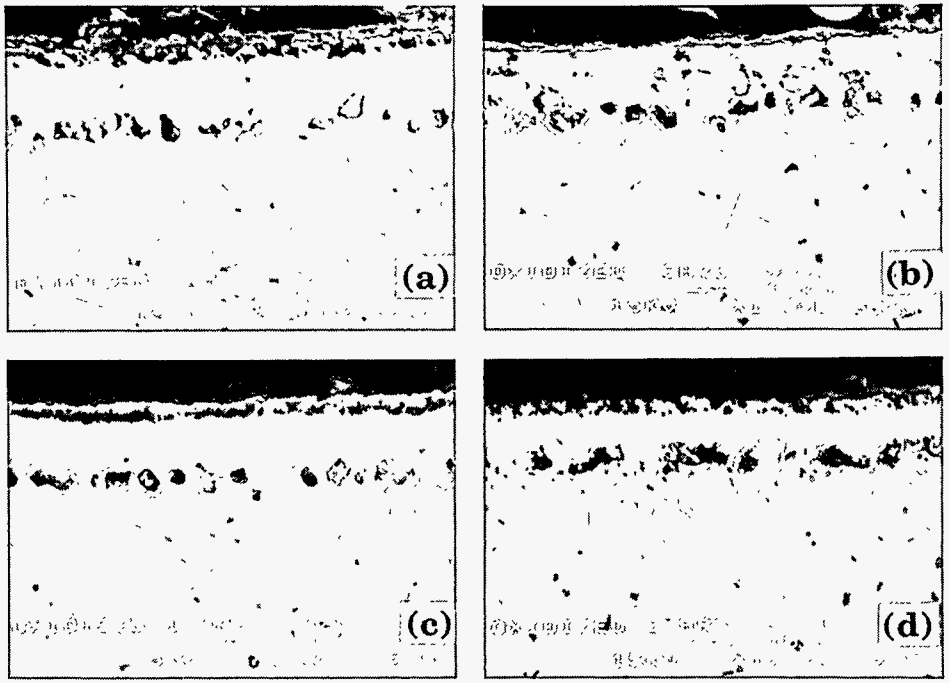

Fig. 3 SEM photomicrographs of specimens of aluminized Type 304 stainless steel pipe oxidized in air at 982°C for different time periods.

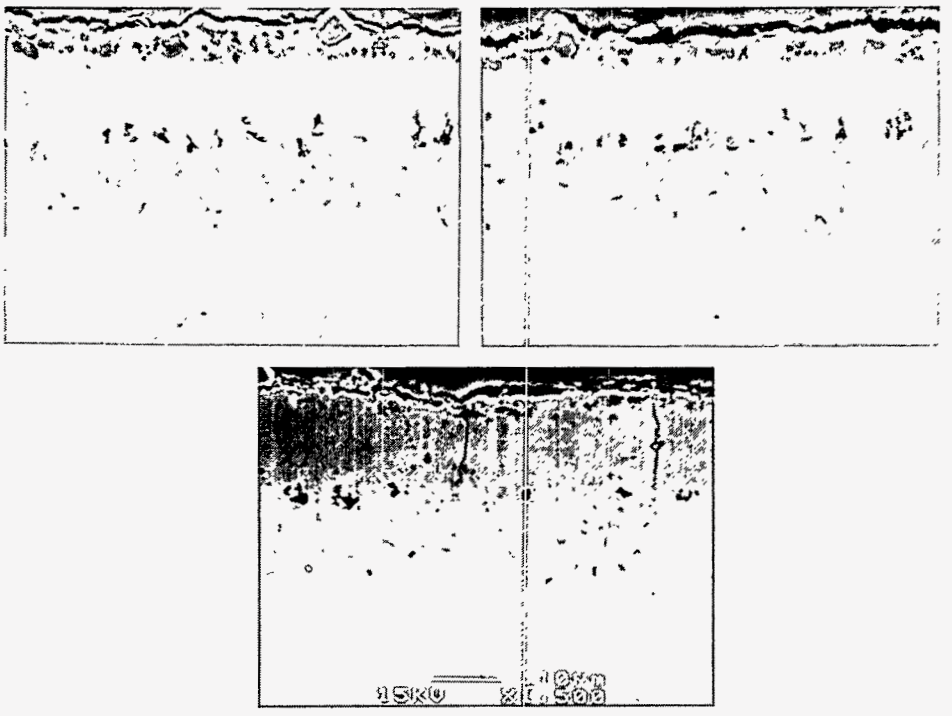

Fig. 4 SEM photomicrographs of three different locations of aluminized Type 304 stainless steel pipe oxidized in air for 4 h at 982°C.

3. Description of Method Used to Produce Test Section Coating

A round pipe of Type 304 stainless steel was aluminized on the inside surface, resulting in a layer of Fe-Al alloy 50-100 μm thick. A commercially available high temperature packed powder process was used. The resultant aluminum rich surface layer was subsequently oxidized in air at 980°C for 4 h, followed by a slow cool in air to room temperature. The end product was a stainless steel tube having an aluminum oxide layer on the inside surface which was a few micrometers thick.

The specific process used, "Alonizing," was performed by ALON Processing, Inc., Tarentum, PA. It is not a coating process; rather, it is a pack cementation process during which aluminum forms intermetallic compounds, in a high temperature vapor phase operation, with the surface layers of the stainless steel substrate. The resultant diffusion zone is resistant to high temperature oxidation, sulfidation, and/or carburization. The exact composition of the pack is proprietary, but it is a mixture of alumina with a fine dispersion of aluminum throughout. Both the alumina and the aluminum particles are extremely fine and as free from foreign materials as is commercially possible.

The inside of the tube was filled with a mixture of the powder; the loaded tube was then placed on its side in a bed of similar powder in a metal retort. The retort was made of 19 mm thick carbon steel and measured approximately 1 m × 1 m × 15 m in length. When the retort was filled with pieces to be Alonized and the processing powder, the top was welded on and two of these vessels were placed in a furnace side by side.

The retorts were heated somewhat beyond 950°C, at which temperature the aluminum component in the powder mix vaporizes and, with the aid of a proprietary activator, diffuses into the inside surface of the pipe creating the characteristic Alonized surface.

After remaining at temperature for more than 24 h, the furnace was turned off. The retort was cooled at a proprietary rate, to a temperature below the lower transformation range (approximately 590°C) at which point the retorts were removed from the furnace and allowed to cool to room temperature on the floor of the shop. The entire cooling process required about 2 days. When cool, the tops

of the retorts were cut off, the pieces removed, and the powder blown from the surface of the pipe.

The mechanism by which the Alonized surface is made resistant to oxidation, sulfidation, and/or carburization is essentially the same as is found with aluminum and its alloys in general, i.e., a very thin film (of the order of a few microns) of aluminum oxide forms on the surface of the Alonized materials and this is a self healing film which is inert in many environments.

An oxide layer thickness approaching 10 μm is considered necessary to produce acceptable ITER relevant conditions. This is based on electrical resistivity values of bulk aluminum oxide, and a margin of three orders of magnitude above the performance requirement to accommodate possible degradation by radiation effects. To achieve this increase (from a few micrometers to approximately 10 μm) the Alonized pipe was suspended in a vertical electric gantry furnace at 980°C for 4 h. The furnace belonged to Lindberg Heat Treating Co., Melrose Park, IL. The heated cavity was 1.8 m in diameter by 7.3 m high. The furnace environment was air at atmospheric pressure; a small air flow (~0.35m^3 s^{-1}) was maintained to favor oxidation over nitridation. Following the four hour heat treat at 980°C, the pipe was cooled to 370°C at less than 100°C h^{-1}; below 370°C, the pipe was allowed to cool in ambient air by natural convection.

4. Description of Test Section

The physical dimensions of the test section were very similar to a previous conducting wall round pipe test section used at ALEX [3,4]. Pressure taps were provided for measuring the axial pressure gradient over a distance of 152.4 mm (2.81 times the pipe radius), the overall pressure drop across the entire magnet including the inlet and outlet fringing fields, and the transverse pressure difference within a cross section. The transverse pressure difference is zero in fully developed flow and arises as a result of axial currents which are created near the fringing fields of the magnet. Two flanges for introducing traversing probes were also provided, see Figs. 5a and 5b. The combination of two flanges and the pressure taps permits the acquisition of data at the inlet, outlet, and within the uniform field region of the magnet. Figure 5b shows the layout of the

instrumentation penetration cluster from which the pressure measurements reported here were collected.

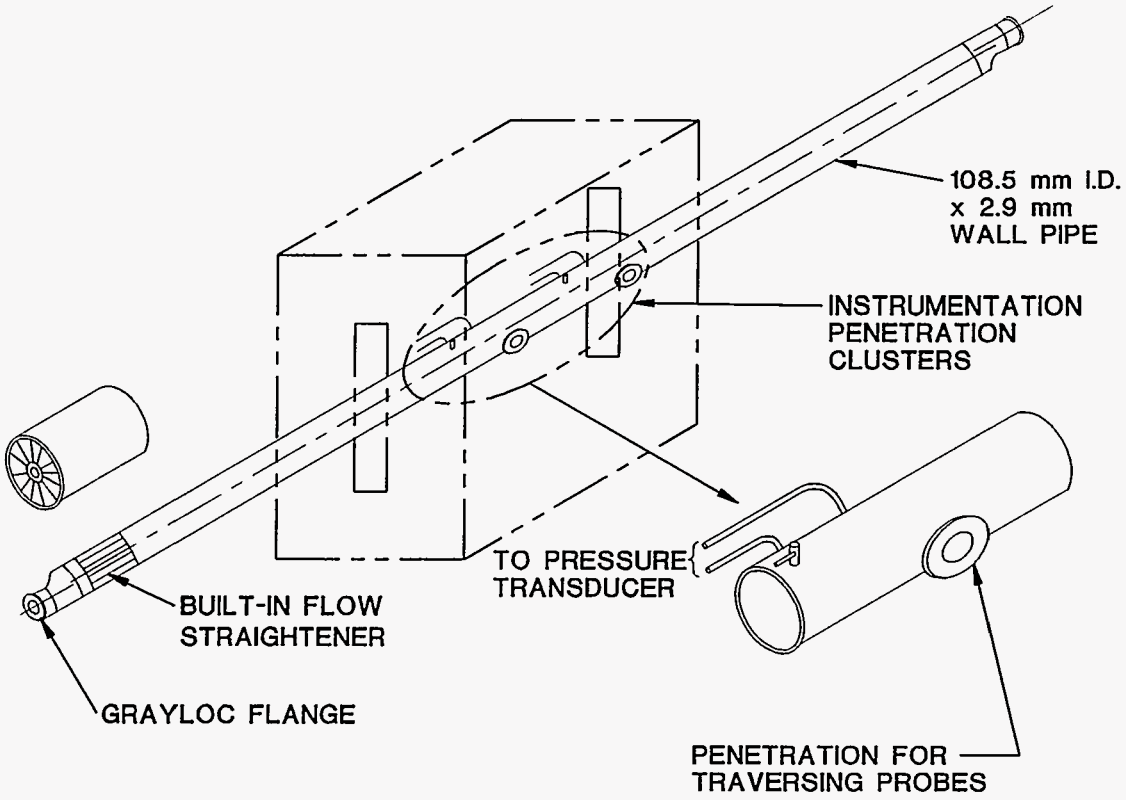

Fig. 5a ALEX insulated pipe test section.

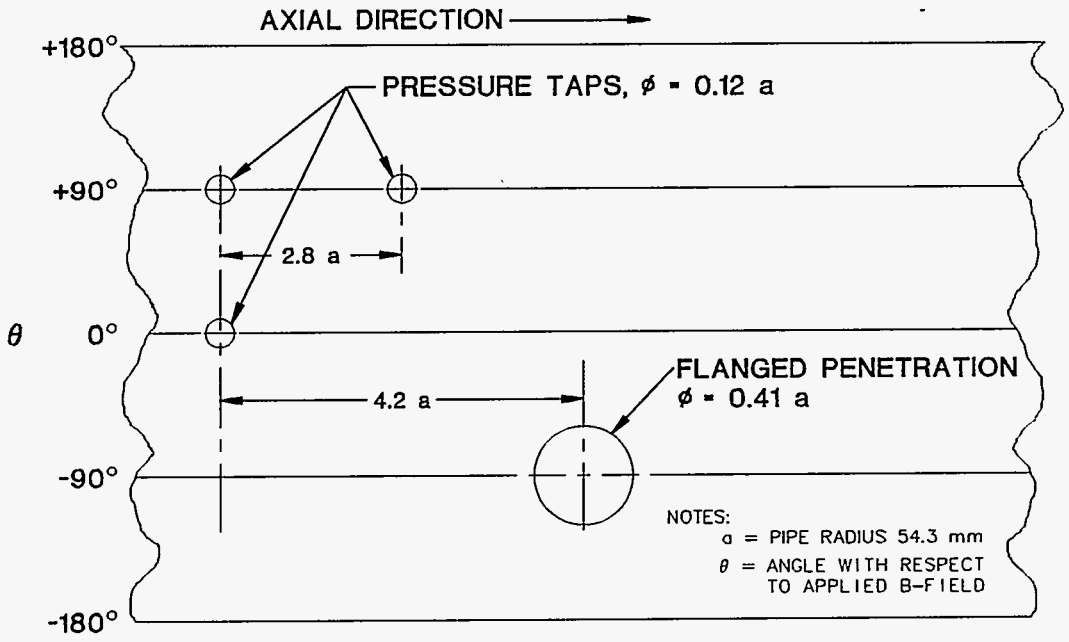

Fig. 5b Instrumentation penetration details.

A movable electrode assembly was fabricated and tested for the first time on this test section. The concept of a movable electrode device was demonstrated in previous tests on a square duct at ALEX. In those tests, a single row of electrodes was constructed and successfully used. In the present tests, a multiple-row assembly of movable electrodes was used, see Figs. 6a and 6b. The movable electrode assembly was made from a fiberglass tube, the inside diameter and wall thickness of which were 127. mm and 12.7 mm, respectively. The movable electrode assembly had six rows of nine electrodes each. The six rows of electrodes were spaced one characteristic length (i.e., pipe radius) apart axially, thus enabling the determination of coating quality and integrity over a section of the pipe extending five characteristic lengths in the axial direction. Voltage distributions which were the result of current flowing in the walls of the test section could be detected.

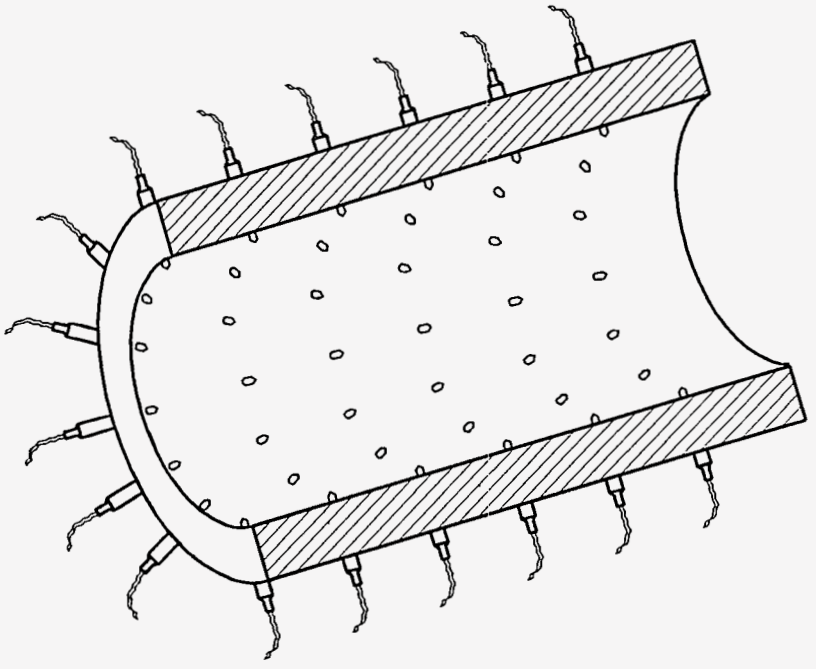

Fig. 6a ALEX insulated pipe movable electrodes.

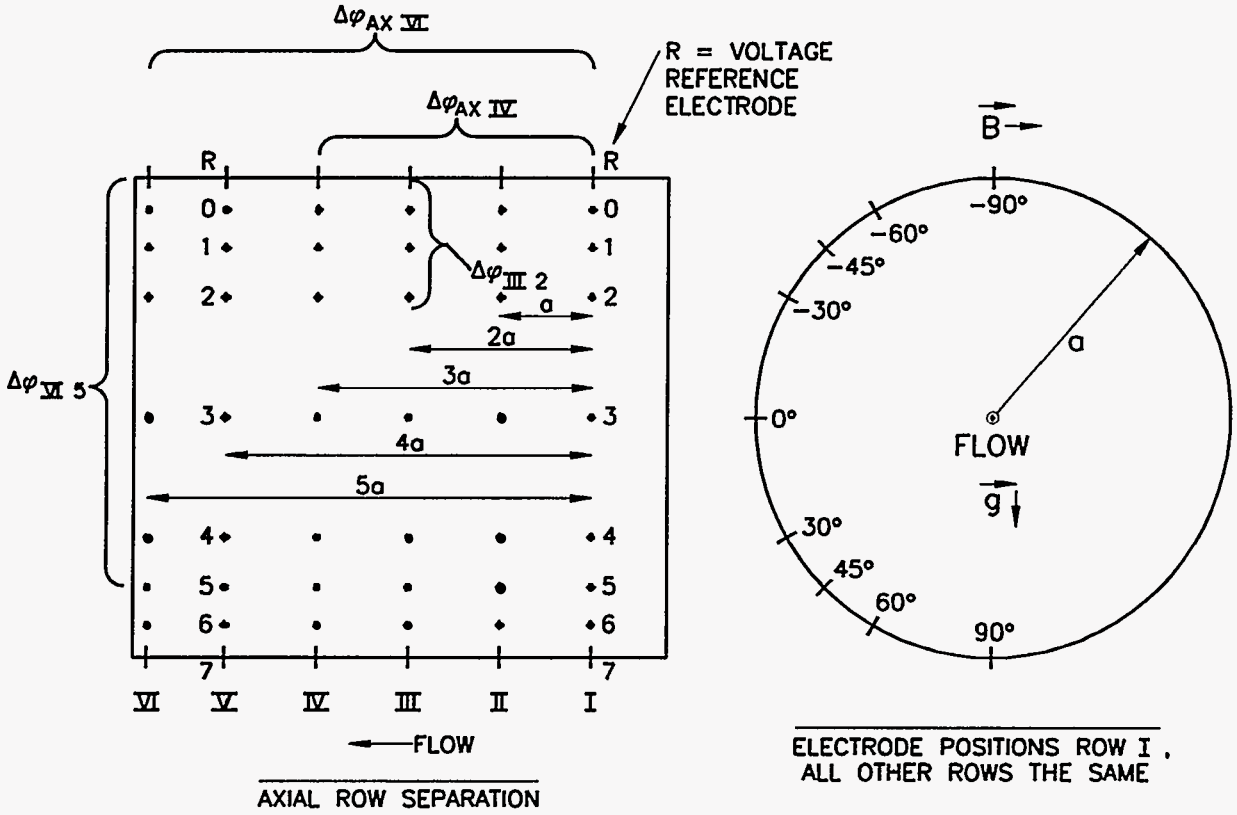

Fig. 6b ALEX insulated pipe movable electrodes, details.

5. Description of Test Conditions and Measurements

Data were taken at five magnetic field strengths (0.0, 0.5, 1.0, 1.5, and 2.0 T) yielding a maximum Hartmann number of 9200. An average NaK velocity of approximately 6.5 cm s^{-1} was used; producing a maximum interaction parameter of 10^4. Three bulk fluid temperatures, 30, 85, and 200°C were attained.

The overall pressure drop across the entire magnet, including the three-dimensional pressure drop caused by the fringing field on each end of the magnet, was determined by measuring the differential pressure between pressure taps located on each end of the test section, very far away from the magnet and its fringing field. This simple measurement was used as the primary indicator of gross reduction in pressure drop due to the presence of the coating. Also, the following measurements were made both within the uniform field and in the fringing field: local axial pressure gradient; local transverse pressure

difference; circumferential and axial voltages on the outside surface of the test section.

The local pressure measurements were acquired by connecting a pair of pressure taps to the pressure transducer system and then moving the magnet to expose the pressure taps to the uniform, fringing, and zero field regions. The voltage measurements were acquired in the same manner, simultaneously with the local pressure measurements. The speed of the magnet motion was approximately 1/25th of the average NaK velocity.

The NaK bulk temperatures of 85 and 200°C were attained by heating the NaK in the dump tank to roughly 25°C above the desired final temperature, filling the loop with the hot NaK, and then circulating the liquid until a quasi-equilibrium temperature was reached. The NaK, the loop piping, and the test section were maintained within 5°C of the desired final temperature for several hours while the data were acquired.

6. Results

Figure 7 shows the overall gross pressure drop across the magnet and fringing fields on each end; data for 30, 85, and 200°C are presented. The lowest curve in the figure is the theoretical prediction of the measurement for a perfectly insulated duct, including the three-dimensional pressure drop coming from the fringing fields, Hua and Walker [5]. The upper curve in the figure (a flat, horizontal line) is the theoretical value of the measurement for a round duct having the same wall thickness as the present test section, but having no insulating coating, i.e., for a bare-wall pipe. The measurements are far below the bare-wall value, indicating that the coating is doing an effective job. The increase of the measurements above the predicted values for perfect insulation may result from two effects: (a) non-perfect electrical insulation as a whole, or (b) the presence of pressure tap and LEVI flange penetrations within the magnetic field. We believe that the second reason is the main factor in these experiments. These penetrations expose the liquid metal to the wall, providing current paths between the liquid metal and the wall. Currents flow from within the liquid metal, through the penetrations, into the wall of the test section, and finally back into the fluid through one of the other penetrations to produce a local axial MHD pressure gradient of the same order as that found in a bare-wall pipe.

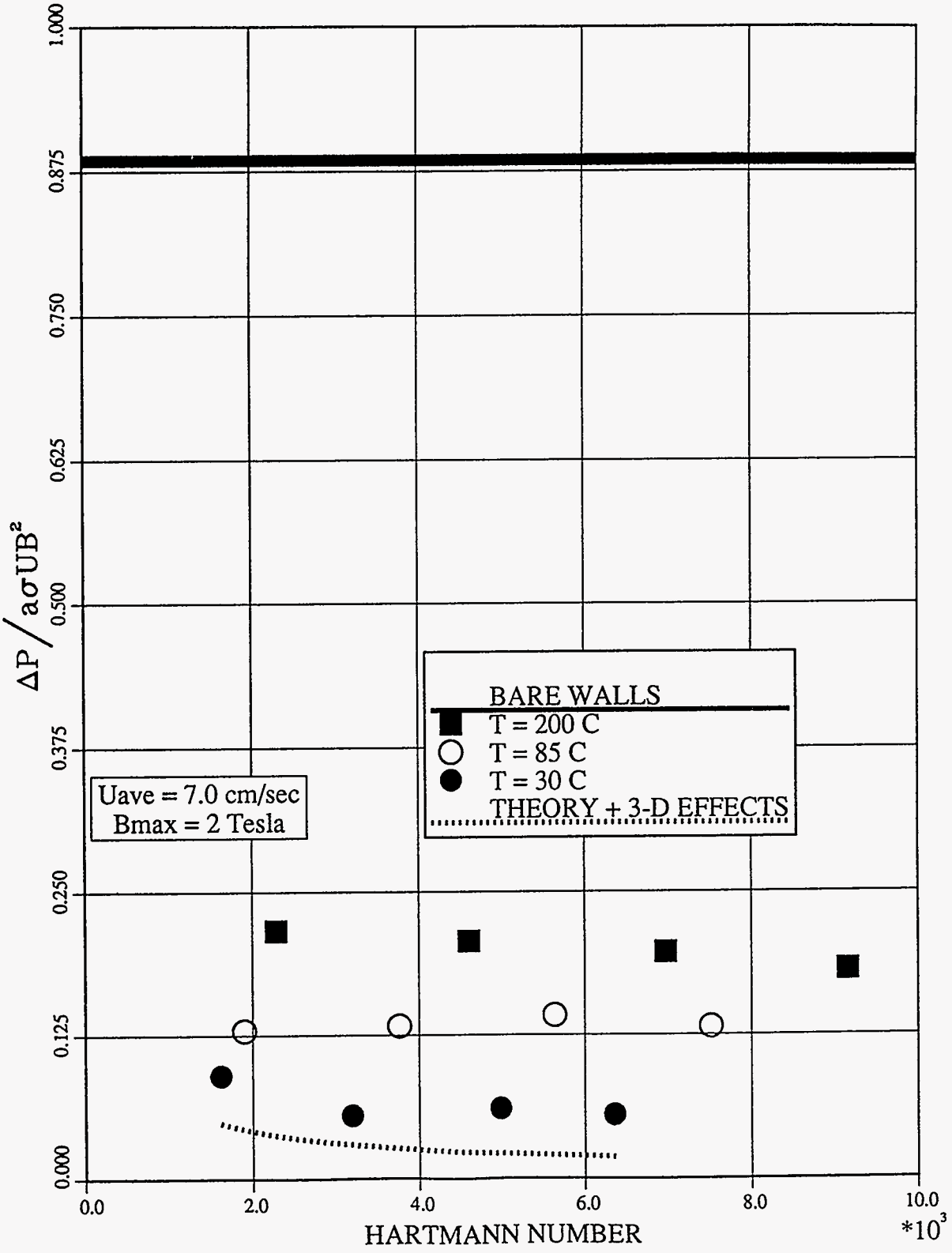

Fig. 7 Insulated pipe overall MHD pressure drop.

This can be seen in Fig. 8, which shows measured axial pressure gradient distributions as a function of the dimensionless axial coordinate, X, for temperatures 85 and 200°C; the B-field distribution and the theoretical axial pressure gradient distribution for a bare-wall pipe are superimposed for reference. The data in Fig. 8 are normalized by the pipe radius, a, instead of the usual axial separation between the pressure taps, so that comparisons between the data in Figs. 7 and 8 are straightforward. Hence, for the remaining discussion, we will speak about dimensionless pressure drops per unit of pipe radius. We can see from Fig. 8 that, within the uniform field region, a pressure drop between the two axial pressure taps of roughly 0.06-0.065 was measured. If one assumes that each of the two instrumentation penetration clusters contributes a pressure drop approximately equal to 0.065 [actually somewhat more, because of the flange penetration, say 4.2/2.8 = 1.5 times 0.065; 4.2 a is the axial length of the instrumentation penetration cluster, see Fig. 5(b)], then the sum of these two pressure drops, plus any pressure drop coming from the remaining well-insulated lengths of the test section inside the uniform field region of the magnet, should add up to the overall MHD pressure drop shown in Fig. 7. However, the position of the magnet during the acquisition of the data in Fig. 7 was such that only part of each of the two penetration clusters was in the uniform field region (one on each end of the magnet), and hence each penetration cluster contributed a pressure drop somewhat less than (1.5×0.065). Finally then, the sum of these two pressure drops (say 0.065 + 0.065) was primarily responsible for the difference between the measurements in Fig. 7 and the perfectly insulating curve at the bottom of the figure. This scenario leads to the conclusion that the Al_2O_3 coating was doing a very good job indeed, because there was more than enough pressure drop coming from the two instrumentation penetrations alone, to account for the measurements in Fig. 7.

The data can also be examined from another viewpoint. If we multiply the value of 0.065 obtained from Fig. 8 by the ratio of the length of the uniform magnetic field region (1800 mm) to the pressure tap separation (152.4 mm), we obtain a value of the overall MHD pressure drop, $dp = 0.065 \times 1800/152.4 \sim 0.8$ which is very close to the bare-wall value shown in Fig. 7.

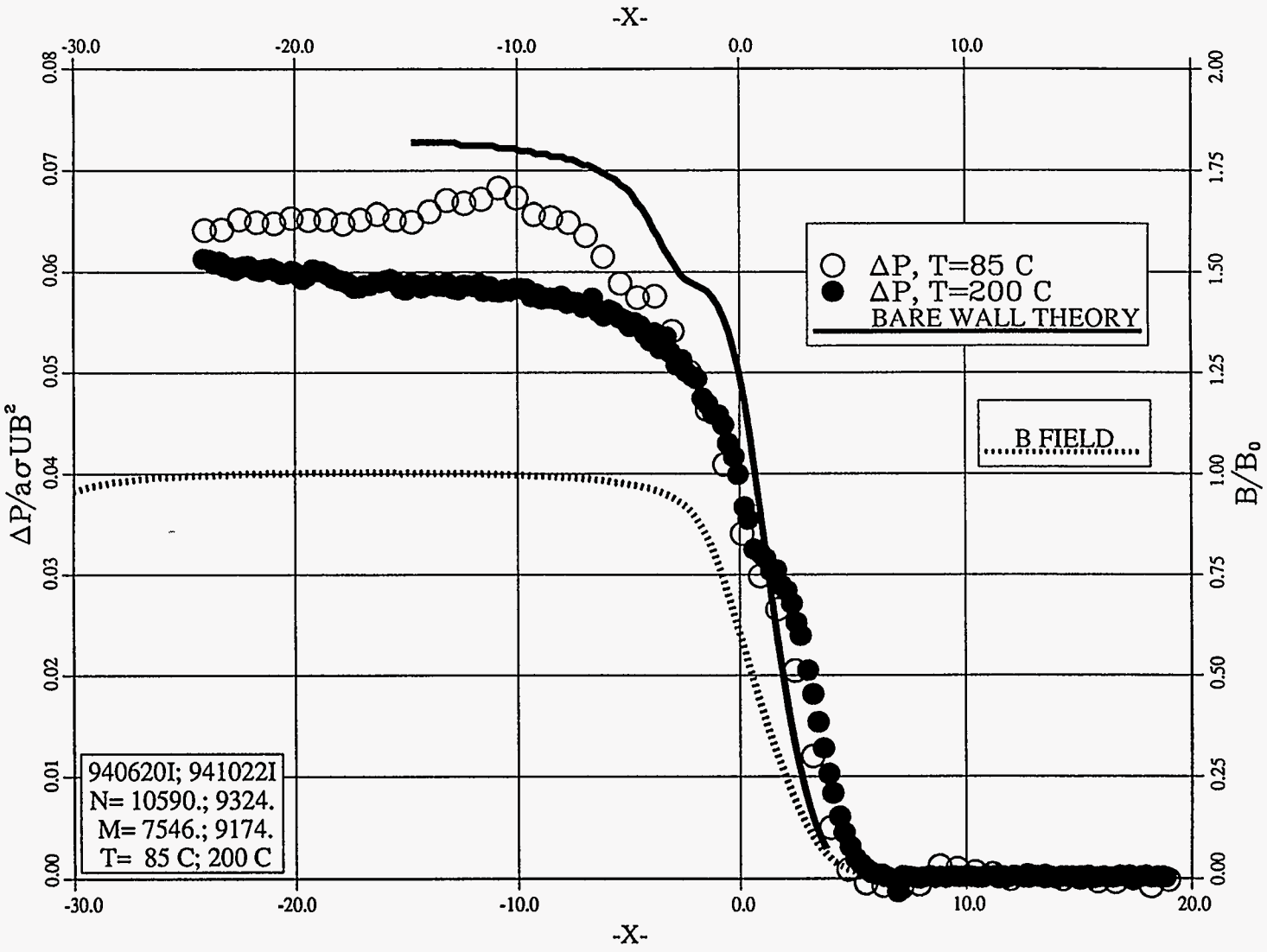

Fig. 8 Axial pressure gradient, insulated pipe.

Further data in support of this hypothesis can be found in Fig. 9, which shows the transverse pressure difference at the upstream edge of the first penetration cluster for T=85 and 200°C. The peak value measured, 0.025-0.035, is only roughly two-thirds of the corresponding value found in a bare-wall pipe. The currents which are responsible for this transverse pressure difference are axial currents. Assuming a good coating, the return path of these axial wall currents to the liquid metal is determined by the separation of the penetrations. Consequently, the electric resistance in the circuit is larger and current magnitudes are smaller than in the bare-wall case.

Figure 10 shows the axial distribution of normalized voltages from the nine electrodes in row 1 of the movable electrode device, in both the uniform and fringing field regions. This row of electrodes was 5.4 pipe radii downstream of the LEVI flange. The magnitude of the highest voltage shown in the figure is roughly 25 times smaller than the bare wall value. Figure 11 shows similar data taken from row 4 of the movable electrode device, 8.4 pipe radii downstream of the LEVI flange; Fig. 11 shows that at this further downstream location, almost no currents flow, except in the fringing region. The trend shown by the other rows in the movable electrode device is to lower voltages as we move further away from the disturbance caused by the nearby penetration cluster. At the furthest row away, 10.4 pipe radii downstream, there is virtually no current flow in the walls of the test section. These electrode data support the claim that the Al_2O_3 coating is intact everywhere except where the instrumentation penetrations have breached it.

Finally, Fig. 12 shows axial distributions of axial surface voltage differences measured between rows of the movable electrode device for T=85 and 200°C. An electrode in the upstream most row was the reference electrode for this figure. The voltages here were normalized by the axial separation of the two electrodes involved. Again, the magnitudes of the voltages are roughly the same or smaller than the circumferential voltages in Figs. 10 and 11, confirming that axial currents are also 25 or more times smaller than the bare wall case.

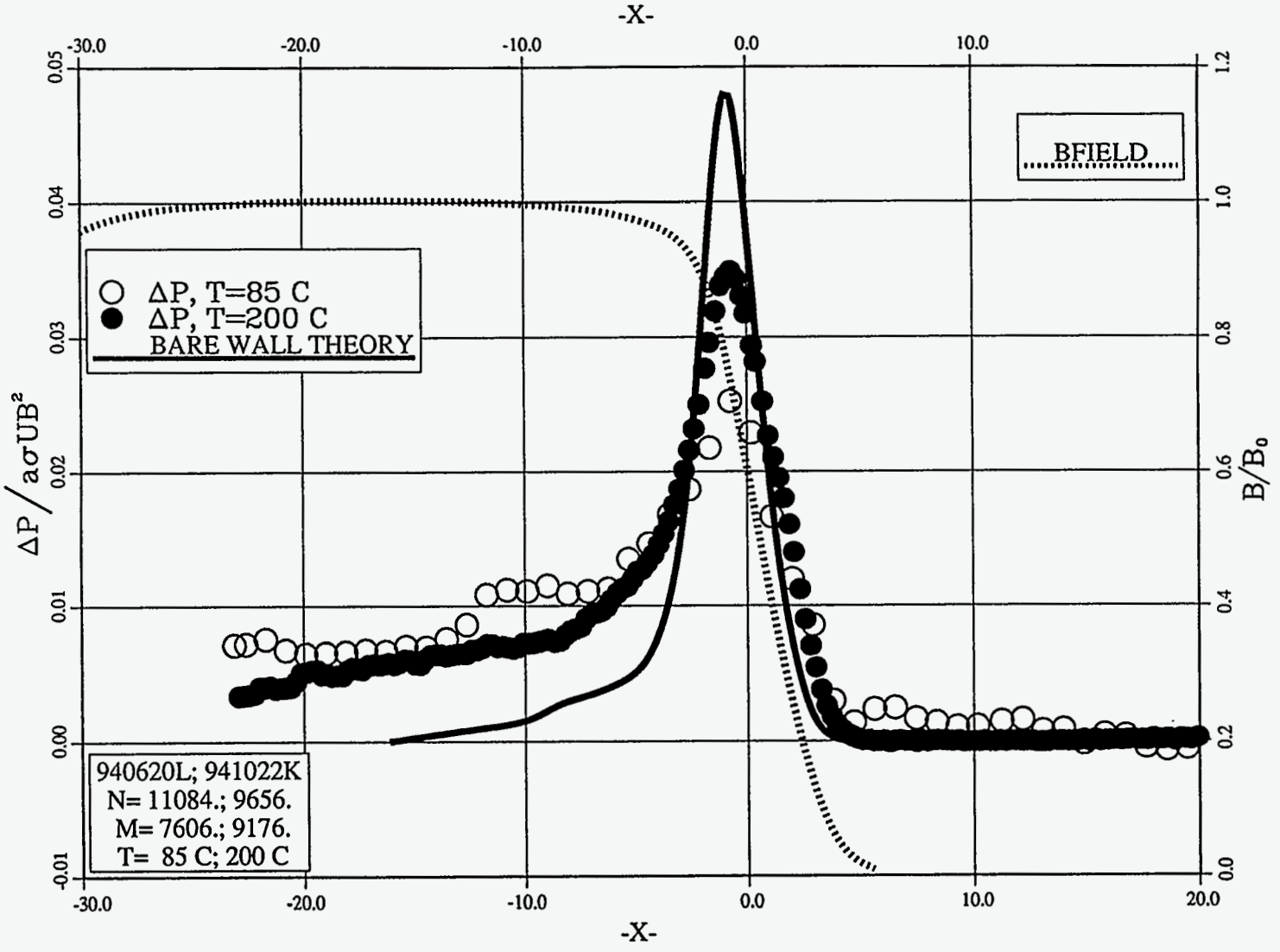

Fig. 9. Transverse pressure difference, insulated pipe.

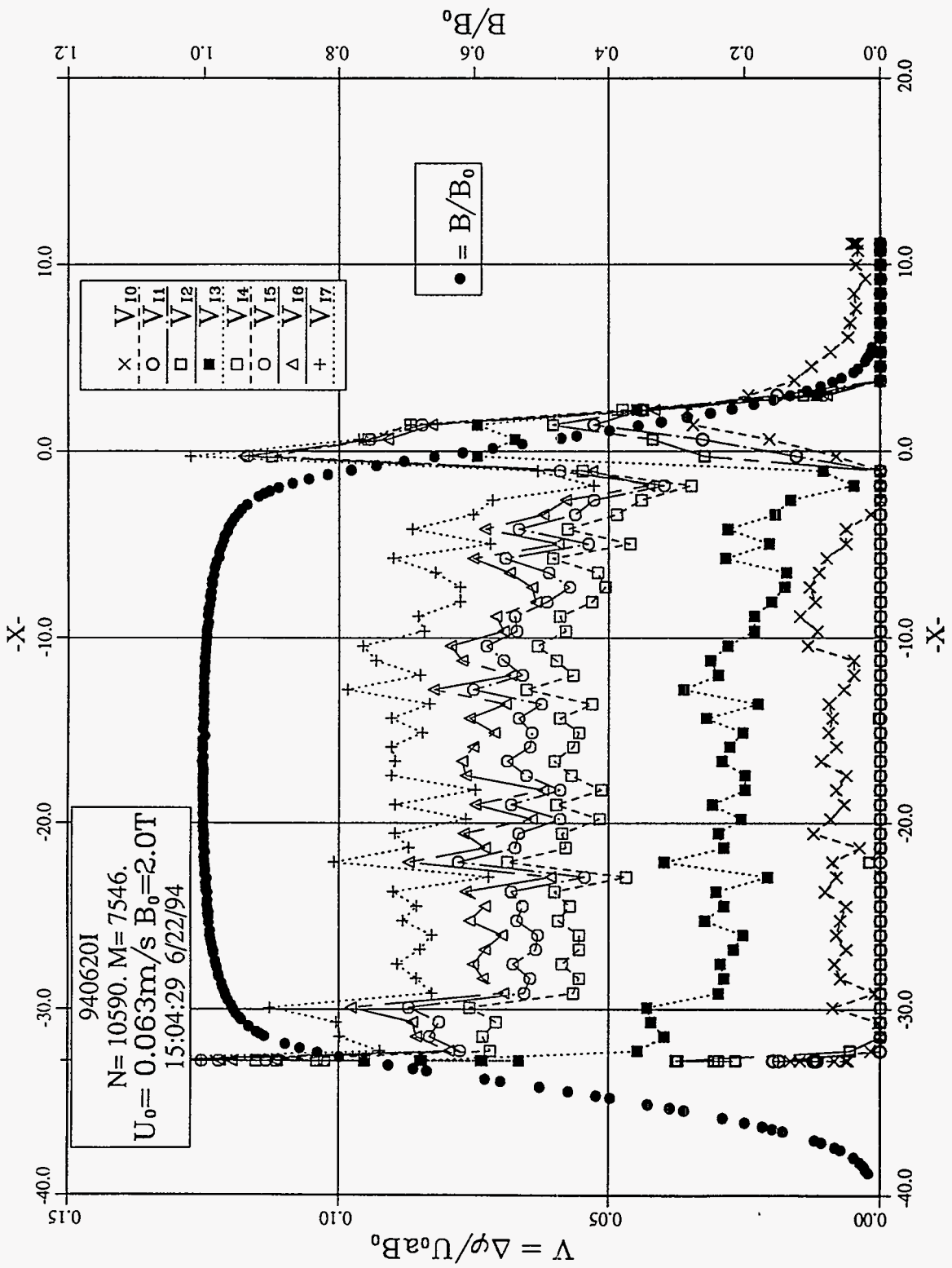

Fig. 10 Circumferential movable electrode voltages, row 1, insulated pipe.

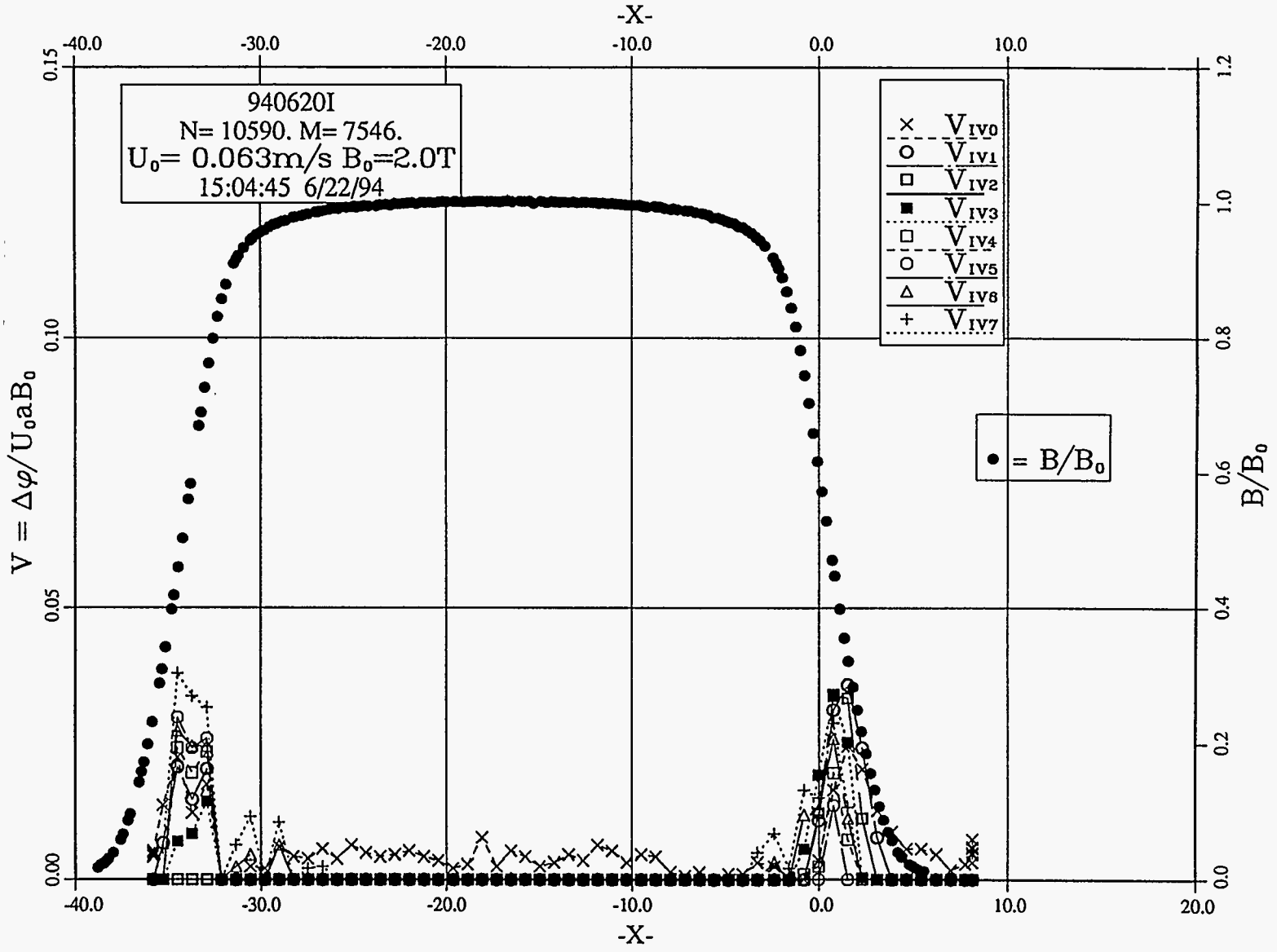

Fig. 11 Circumferential movable electrode voltages, row 4, insulated pipe.

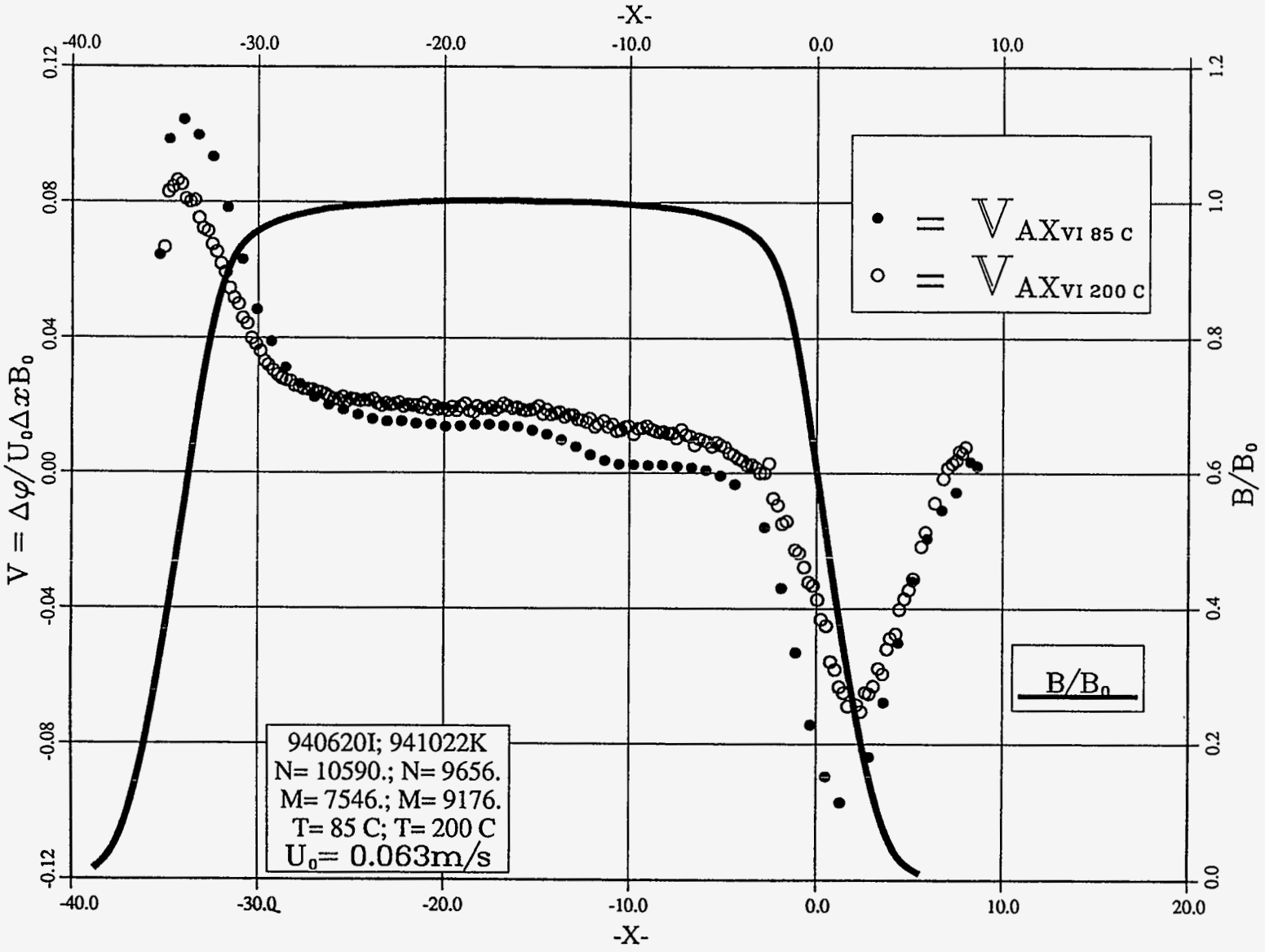

Fig. 12 Movable electrode axial voltages, insulated pipe.

The hypothesis that the penetration clusters are largely responsible for the discrepancy between the theory and the data in Fig. 7 is consistent with the increase in MHD pressure drop noted as the temperature was increased from 30 to 85 to 200°C. This is because the wetting action of NaK increases as the temperature increases, thus reducing the electrical contact resistance on the uncoated stainless steel surfaces of the instrumentation penetrations, leading to higher current flow into the walls (NaK generally does not fully wet stainless steel below 300°C). It is important to note that, according to Fig. 12, there was little effect of temperature on the axial currents flowing in the walls of the pipe far away from the penetration clusters (10.4 pipe radii downstream of the LEVI flange). This figure would most clearly indicate a failed coating with high levels of axial surface voltages; but none of significance were detected.

7. Implications for ITER

The positive results obtained here for high-temperature NaK have two beneficial implications for ITER. First, since NaK may be used in the vacuum vessel and/or the divertor, these results support the design approach of using electrically insulating coatings to substantially reduce MHD pressure drop. Electrically insulating coatings are, therefore, no longer a feasibility issue in these two components.

Secondly, while Al_2O_3/SS is not the same coating/base material combination which would be used in the advanced blanket, this work nonetheless shows that it is possible to produce a viable insulating coating which is stable in contact with a high temperature alkali metal coolant. Also, it was demonstrated that such coatings can be formed on large scale components, in this case 10.8 cm in diameter, using commercially available industrial equipment and processes.

8. Conclusions

A round pipe test section, coated on the inside surface with Al_2O_3, was fabricated and tested in ALEX. NaK temperatures of 200°C were reached. Measurements were made of the overall gross MHD pressure drop, local axial pressure gradient, local transverse pressure difference, and axial and circumferential surface voltage distributions. Hartmann numbers reached 9200, and interaction parameters reached 10^4. Overall gross MHD pressure drops

were higher than perfectly insulated values, but many times lower than bare-wall values. Local measurements of pressures and voltage distributions showed that the presence of the instrumentation penetrations themselves caused the higher values of the overall gross MHD pressure drop.

Acknowledgments

The authors wish to thank Mr. Robert C. Haglund for his dedication and hard work in installing the test section and in operating the ALEX facility. This work was supported by the US Department of Energy, Office of Fusion Energy, under Contract W-31-109-Eng-38.

References

[1] T. Q. Hua and Y. Gohar, "MHD Pressure Drops and Thermal Hydraulic Analysis for the ITER Breeding Blanket," this conference.

[2] K. Natesan, C. B. Reed, and R. F. Mattas, "Assessment of Alkali Metal Coolants for the ITER Blanket," this conference.

[3] B. F. Picologlou, C. B. Reed, P. V. Dauzvardis, and J. S. Walker, "Experimental and Analytical Investigations of Magnetohydrodynamic Flows Near the Entrance to a Strong Magnetic Field," Fusion Technology 10(3), 860-865 (1986).

[4] C. B. Reed, B. F. Picologlou, T. Q. Hua, and J. S. Walker, "ALEX Results - a Comparison of Measurements from a Round and a Rectangular Duct with 3-D Code Predictions," Proceedings of the 12th Symposium on Fusion Engineering, pp. 1267-1270, October, 1987.

[5] T. Q. Hua and J. S. Walker, "Three-Dimensional MHD Flow in Insulating Circular Ducts in Non-uniform Transverse Magnetic Fields," Int. J. of Engr. Science 27 (1989) 1079.

DISTRIBUTION LIST FOR ANL/FPP/TM-281

Internal

H. Attaya
S. Bhattacharyya
M. Billone
J. Brooks
H. Chung
D. Ehst
Y. Gohar
A. Hassanein
T. Hua
C. Johnson
T. Kassner
M. Lineberry
S. Majumdar
R. Mattas
K. Natesan
J.H. Park
C.B. Reed (9)
Dale L. Smith
D.-K. Sze
H. Tsai

FPP Files (5)
TIS Files (1)

External

DOE/OSTI for distribution per UC-424 (41)
Manager, Chicago Operations Office
ANL-E Libraries (2)
ANL-W Library
M. Abdou, University of California, Los Angeles
K. Abe, Tohoku University, Japan
A. Anisimov, Efremov Institute, St. Petersburg, Russia
C. Baker, University of California, San Diego
L. Barleon, Forschungszentrum Karlsruhe, Germany
S. Berk, U.S. Department of Energy
H. Bolt, Institute for Materials in Energy Systems - IWE, Germany
L. Bühler, Forschungszentrum Karlsruhe, Germany
R. Causey, Sandia National Laboratories, Livermore
M. Cohen, U.S. Department of Energy
W. Daenner, ITER, Germany
J. Doggett, Lawrence Livermore National Laboratory
W. Gauster, ITER JCT, Garching, Germany
J. Hunter, Sandia National Laboratories, Albuquerque
T. James, University of California, San Diego
K. Ioki, ITER JCT, Germany
Y. Kato, Japan Atomic Energy Research Institute, Japan
I. Kirillov, Efremov Institute, St. Petersburg, Russia
O. Lielausis, Institute of Physics, Latvia
S. Malang, Forschungszentrum Karlsruhe, Germany
Y. Martynenko, Kurchatov Institute, Russia
K. McCarthy, Idaho National Engineering Laboratory
J. McWhirter, Idaho State University
K. Miya, University of Tokyo, Japan
K. Miyazaki, Osaka University, Japan
Y. Momozaki, Tokyo Institute of Technology, Japan
O. Motojima, National Institute for Fusion Science, Japan
U. Müller, Forschungszentrum Karlsruhe, Germany
E. Muraviev, ITER JCT, San Diego, California

R. Parker, ITER JCT, Garching, Germany
S. Piet, ITER JCT, San Diego, California
R. Price, U.S. Department of Energy
M. Seki, Japan Atomic Energy Research Institute, Japan
Y. Strebkov, RDIPE, Moscow, Russia
M. Tillack, University of California, San Diego
J. Vetter, Forschungszentrum Karlsruhe, Germany
G. Vieider, ITER, Germany
I. Vitkovski, Efremov Institute, St. Petersburg, Russia
J. Walker, University of Illinois, Champaign-Urbana
F.W. Wiffen, U.S. Department of Energy
K. Wilson, Sandia National Laboratories, Livermore
Bibliothek, Max-Planck-Institute fur Plasmaphysik, Germany
C.E.A. Library, Fontenay-aux-Roses, France
Librarian, Culham Laboratory, England
Thermonuclear Library, Japan Atomic Energy Research Institute, Japan